Hydrol. Earth Syst. Sci. Discuss., 6, 4035–4064, 2009
www.hydrol-earth-syst-sci-discuss.net/6/4035/2009/

Hydrology and Earth System Sciences Discussions

Papers published in *Hydrology and Earth System Sciences Discussions* are under open-access review for the journal *Hydrology and Earth System Sciences*

Hourly soil moisture mapping over West Africa using AMSR-E observations and a satellite-based rainfall product

T. Pellarin[1], T. Tran[1], J.-M. Cohard[1], S. Galle[1], J.-P. Laurent[1], P. de Rosnay[2], and T. Vischel[1]

[1]LTHE, CNRS-INSU, Université de Grenoble, BP 53, 38041 Grenoble Cedex 9, France
[2]European Centre for Medium-Range Weather Forecasts, Reading, UK

Received: 21 April 2009 – Accepted: 6 May 2009 – Published: 3 June 2009

Correspondence to: T. Pellarin (thierry.pellarin@hmg.inpg.fr)

Published by Copernicus Publications on behalf of the European Geosciences Union.

Abstract

This paper provides an original and simple methodology to map surface soil moisture with a fine temporal and spatial resolution over large areas based on a satellite rainfall accumulation product and soil microwave emission measurements at C-band. The first motivation of this study was to obtain high temporal frequency (~1 h) in order to study the possible feedback mechanisms between soil moisture and convection in West Africa. The use of soil moisture maps derived from satellite microwave measurements was not possible due to the low (at best daily) temporal resolution. Thus, a rainfall accumulation product based on Meteosat geostationary satellite measurements was used together with a simple Antecedent Precipitation Index (API) model to produce soil moisture map at the $10 \times 10\,km^2$ and 30 min resolution. Due to uncertainties on the satellite-based rainfall accumulation product, derived soil moisture maps were found to be erroneous. An assimilation technique based on AMSR-E C-band measurements into a microwave emission model was developed. The assimilation technique described in this study consists of modulating the rainfall accumulation estimate between two successive AMSR-E brightness temperatures (TB) measurements in order to match simulated and observed TB. When a rainfall event happens, the initial rainfall accumulation estimate is modulated using a multiplicative factor ranging from 0 to 7. The best solution is given by the rainfall rate which minimizes the difference between observed and simulated TB. Ground-based soil moisture measurements obtained at three sites in Niger, Mali and Benin were used to assess the methodology which was found to improve the soil moisture estimates over the three sites.

1 Introduction

A number of recent papers have focused on studying the potential role of soil moisture in surface-precipitation feedbacks. A large part of these studies concern West Africa where Koster et al. (2004) shown that there is a strong coupling between soil moisture

HESSD

6, 4035–4064, 2009

and precipitation in climate models. The soil moisture-precipitation feedback can be either positive, when the additional atmospheric humidity provided by a wet area tends to generate higher precipitation, or negative when the soil moisture tends to reduce moist convection over wet areas. Taylor et al. (1997) found persistent rainfall patterns in the Sahel suggesting a positive feedback. Similar findings were found with modelling studies (Liu and Avissar, 1999). Conversely, some authors showed negative feedbacks as in Cheng and Cotton, 2004; Taylor and Ellis, 2006; and Cook et al., 2006.

A difficulty in studying soil moisture-precipitation feedback based on observational data is the lack of accurate soil moisture mapping at the spatial and temporal scale suitable with rainfall systems. Today, no satellite sensor has optimal characteristics for soil moisture retrieval. The frequencies and the spatial and temporal resolutions have not been specifically selected for continental studies (Prigent et al., 2005). In the near future, two proposed space missions will be exclusively devoted to measure soil moisture from space; the SMOS mission (Kerr et al., 2001) and the SMAP mission (Entekhabi et al., 2007). At the moment, the AMSR-E sensor onboard the Aqua platform provides passive microwave measurements which are directly related to soil moisture over areas with no or low vegetation cover (Jackson et al., 2008). However, the temporal resolution of AMSR-E (ranging from 12 h to 36 h) was found to be insufficient to capture the rapid dynamic of the surface soil moisture in West Africa (Pellarin et al., 2008). In Sahelian regions (12° N–20° N), most (80–90%) of the rainfall events are convective systems and most of them are short-lived (<10 h) systems (Laurent et al., 1996; Mathon et al., 2002). In addition, warm atmospheric conditions in the Sahel region produce high evaporation rate which dries rapidly the first centimetres of the soil which are observable by satellite microwave sensors.

In this paper, a methodology is proposed to provide high resolution surface soil moisture estimates ($10 \times 10\,km^2$, 30 min) in order to enable statistical studies to further our understanding of the soil-atmosphere feedback. Section 2 describes the methodology based on two satellite-based measurements, a simple Antecedent Precipitation Index (API) model and a microwave emission model. In addition, soil moisture measurements

acquired at the ground level over a North-South gradient (Mali, Niger and Benin) are used to assess the methodology. Section 3 presents the results at the local and the regional scales.

2 Method

The approach is based on the assimilation of AMSR-E microwave brightness temperatures (TB) into a simple Antecedent Precipitation Index (API) model coupled with a microwave emission model. The API model uses a satellite-based rainfall accumulation product (EPSAT-SG) as input and provides 2-D surface soil moisture mapping over West Africa every 30 min. The microwave emission model produces the associated microwave TB at C-band (6.9 GHz). Then, the assimilation technique consists on modulating the satellite-based rainfall accumulation estimates in order to match the simulated TB and the observed AMSR-E TB. The originality of this study is to account for the rainfall uncertainty with a specific assimilation technique.

2.1 EPSAT-SG satellite-based rainfall accumulation product

The EPSAT-SG rainfall product (Chopin et al., 2005) is based on the IR geostationary satellite data provided by METEOSAT 8 and low orbiting satellite microwave data of the Tropical Rainfall Measurement Mission (TRMM) radar, using a neural network procedure. The annual rainfall accumulation is forced to match the Global Precipitation Climatology Project (GPCP) rainfall product (Adler et al., 2003). A comparison of the EPSAT-SG rainfall product with ground-based rainfall measurements acquired over the three sites in Niger, Mali and Benin is shown in Fig. 1. It can be observed that the main sources of discrepancy are due to an overestimation by EPSAT-SG of the total number of rainy days and an underestimation of the rainfall accumulation at the event timescale. The total number of rainy days (from June to September 2006) measured at the ground level in Niger (Wankama site) is 34 whereas the EPSAT-SG detects 86 days. In Mali

(Agoufou site) the number of rainy days is 39 (ground level) and 76 days (EPSAT-SG). In Benin (Nalohou site) the number of rainy days is 51 (ground level) and 97 days (EPSAT-SG). In addition, the total rain amount (from June to September) is underestimated by 37%, 14% and 22% for the Niger, Mali and Benin sites, respectively. On the other hand, it can be observed that each rainfall event measured at the ground level is detected by the satellite-based rainfall product.

2.2 Ground-based soil moisture measurements

In situ soil moisture measurements were obtained using CS616 sensors (Campbell Scientific Inc., Logan, Utah, USA) over three sites located in Niger at Wankama (13.65° N, 2.63° E), Mali at Agoufou (15.35° N, 1.48° W), and Benin at Nalohou (9.75° N, 1.61° E). Soil moisture sensors are located at 5 cm depth. Six soil moisture sensors were installed at the Wankama site, three at the Agoufou site and three at the Nalohou site. A detailed description of these measurements (and the calibration procedure) can be found in de Rosnay et al. (2009a) and Pellarin et al. (2009).

2.3 API model

The API model is described following:

$$\mathrm{API}_j = \mathrm{API}_{j-1} e^{-30/\delta} + P_j \quad (1)$$

where j is a daily time index, Pj an estimate of the rainfall accumulation during 30 min [mm], and δ a decreasing time parameter expressed in minutes. To match the API with observed volumetric soil moisture measurements [v/v], Crow and Ryu (2009) proposed a rescaling procedure following:

$$\theta_j = \left(\mathrm{API}_j - \mu^{\theta}\right)\left(\sigma^{\mathrm{API}} \Big/ \sigma^{\theta}\right) + \mu^{\mathrm{API}} \quad (2)$$

The rescaling procedure ensures that the rescaled soil moisture possess a long-term mean (μ) and standard deviation (σ) matching the observed mean soil moisture (μ^{θ})

HESSD
6, 4035–4064, 2009

and standard deviation (σ^{θ}). However, the mean soil moisture (μ^{θ}) and standard deviation (σ^{θ}) values are available only where in-situ measurements are obtained. To produce 2-D soil moisture mapping over West Africa using the proposed approach, a spatial distribution of μ^{θ} and σ^{θ} is required. To solve this, the use of 6 surface soil moisture time series measured in Mali (Bamba, Zaket, Ekia, Agoufou), Niger (Wankama) and Benin (Nalohou) leaded to find a statistical relationship between μ^{API} and μ^{θ} and a second relationship between σ^{API} and σ^{θ} as shown in Fig. 2. The two relationships can be written as:

$$\mu^{\theta} = 0.0062\,\mu^{\mathrm{API}} \tag{3}$$

$$\sigma^{\theta} = 0.0019\,\sigma^{\mathrm{API}} + 0.0211 \tag{4}$$

2.4 C-band brightness temperatures simulations

The C-MEB (C-band Microwave Emission of the Biosphere) microwave model (Pellarin et al., 2006) was used to simulate brightness temperatures based on 2-D soil moisture mapping obtained in the first step. In the C-MEB model, the polarized brightness temperature (TB_p) is written as a function of the ground emissivity (e_p) and the effective soil temperature (T_{eff}) as $TB_p = e_p . T_{\mathrm{eff}}$. The ground emission is computed as $e_p = 1 - r_p$, where r_p is the polarized microwave reflectivity which mainly depends on soil moisture and, to a small extent, soil density, and textural and structural properties (Wigneron et al., 2007). To model the soil reflectivity, the approach is based on the generalized semi-empirical formulation developed by Wang et al. (1983), based on three roughness parameters h_{soil}, q_{soil} and N_{soil}:

$$r_p(\theta) = \left[(1 - q_{\mathrm{soil}})\, r_p^*(\theta) + q_{\mathrm{soil}} r_q^*(\theta)\right] \exp\left(-h_{\mathrm{soil}} \cos^{N_{\mathrm{soil}}}(\theta)\right) \tag{5}$$

where θ is the incidence angle and r_p^* is the soil reflectivity of a plane surface which depends on the soil dielectric permittivity and the incidence angle. Wang et al. (1983) found that $N_{\mathrm{soil}}=0$ was consistent with measurements at three frequencies (1.4, 5,

HESSD
6, 4035–4064, 2009

and 10.7 GHz). Concerning the soil dielectric permittivity, two studies devoted to West Africa showed that the Mironov model (Mironov et al., 2004) is suitably designed for African areas (Pellarin et al., 2009; de Rosnay et al., 2009b).

A simple parameterization of the effective soil temperature was introduced by Wigneron et al. (2001) as a function of the soil temperature at two depths and the surface soil moisture as:

$$T_{\text{eff}} = T_{\text{deep}} + \left(wg/w_0\right)^{bw_0} \left(T_{\text{surf}} - T_{\text{deep}}\right) \quad (6)$$

where wg is the surface soil moisture, w_0 and bw_0 are semi-empirical parameters depending on the specific soil characteristics, T_{surf} and T_{deep} are the soil temperatures at 1 cm and 50 cm depth, respectively. At the regional scale, surface soil temperatures were provided by the SEVIRI/MSG geostationary satellite and were processed by the LSA-SAF operational node at the Institute of Meteorology of Portugal. In cloudy conditions, missing surface soil temperatures were replaced by modelled surface soil temperatures derived from the ISBA land surface model (Noilhan and Planton, 1989). Atmospheric fields required by ISBA were provided by the ALMIP Intercomparison Project (http://www.cnrm.meteo.fr/amma-moana/amma_surf/almip/index.html and Boone et al., 2009). Similarly, deep soil temperature values were also derived from ISBA land surface model. Note that the deep soil temperature had a low influence relatively to soil emissivity.

When a vegetation layer is present over the soil surface, it attenuates the soil emission and adds its own contribution to the emitted radiation. At low frequencies, these effects can be well approximated by a simple semi-empirical model, referred to as the $\tau - \omega$ model. This model is based on two parameters, the optical depth τ and the single scattering albedo ω, which are used to parameterize, respectively, the vegetation attenuation properties and the scattering effects within the canopy layer (Mo et al., 1982). Based on the $\tau-\omega$ approach several parameterizations have been proposed to compute the vegetation optical thickness. In West Africa, de Rosnay et al. (2009b) showed that the best parameterization was the Kirdyashev formulation (Kirdyashev et

al., 1979). It expresses the vegetation optical thickness as a function of the wave number k (between 1 GHz and 7.5 GHz), the dielectric constant of vegetation water ε''_{vw} (imaginary part), VWc, incidence angle θ, water density ρ water and a vegetation structure parameter a_{geo}:

$$\tau_{veg,p} = a_{geo}.k.\frac{VWc}{\rho_{water}}.\varepsilon''_{vw}.\frac{1}{\cos\theta} \quad (7)$$

The vegetation water content (VWc) was derived from leaf area index (LAI) provided by the ECOCLIMAP database (Masson et al., 2003).

2.5 Assimilation of AMSR-E microwave measurements

The assimilation technique proposed in this study assumes that the rainfall rate is possibly erroneous (as shown in Fig. 1) and could be adjusted by changing the rainfall rate using a simple multiplicative factor. This yields to modify the surface soil moisture and the associated simulated brightness temperatures. The best solution is obtained for the lower difference between observed (AMSR-E) and simulated TB in term of root mean square errors (RMSE). The sequential algorithm is based on two successive AMSR-E TB measurements over a given pixel, and computes eight soil moisture simulations using the following multiplicative factors: 0, 0.25, 0.5, 1, 2, 3, 5 or 7. Figure 3 shows an example of the eight simulated soil moisture time-series between two successive AMSR-E TB measurements. The second graph presents the simulated TB associated with the eight soil moisture simulations. The best solution is given by the soil moisture simulation which provides the closer TB simulation and TB observations. In Fig. 3, the best solution is given by the multiplicative factor 2.

3 Results

3.1 API model at the locale scale

The API technique was assessed at the locale scale using ground-based rainfall measurements and satellite-based rainfall estimates. A calibration procedure was done to find the best decreasing time parameter δ of Eq. (1) for the three sites of Wankama (Niger), Agoufou (Mali) and Nalohou (Benin). A value equal to 4 days (δ=5760 min) was fitted to be relevant for the three sites. Comparisons were done using the mean value of all soil moisture measurements (−5 cm) located around Wankama (6 sensors), Agoufou (3 sensors) and Nalohou (3 sensors).

When ground-based rainfall measurements are used, the coefficients of determination (R^2) are equal to 0.69, 0.63 and 0.50 at the Wankama, Agoufou and Nalohou site, respectively. The total number of rainy days from June 1st to 30 September is also mentioned in Fig. 4 (a rainy day corresponds to a 24-h period where a rain event occurs).

When satellite-based rainfall estimates (EPSAT-SG) are used, the agreement (R^2) between observed and estimated soil moisture decreased from 0.69 to 0.28 at Wankama, from 0.63 to 0.36 at Agoufou, and from 0.50 to 0.46 at Nalohou. Lower scores are mainly due to the strong underestimation of the rainfall accumulation at the beginning of the rainy season (June to mid-July) and the overestimation of the number of rainy days. Untrue rainy events can be easily observed at the Wankama site at the beginning of July and at the end of September. Despite that, due to the normalization procedure presented in Sect. 2.3, the methodology provides surface soil moisture estimates with a low bias (<1.6% vol.) and relatively low RMSE (<3.7% vol.).

3.2 Microwave brightness temperatures at the regional scale

Based on the EPAST-SG rain accumulation product (10×10 km^2, 30 min), soil moisture maps at the same spatial and temporal resolution were performed using Eqs. (1) to

(4) at the regional scale. To compute microwave brightness temperatures, the ECOCLIMAP database is used to differentiate three kinds of land covers (bare soil, forest and herbaceous vegetation) as shown in Fig. 5. The vegetation water content (VWc) values were fixed to 4 kg/m^2 for forest tile and 0.5×LAI for herbaceous vegetation (Pellarin et al., 2003) with LAI derived from the ECOCLIMAP database. The a_{geo} parameter value is fixed to 0.66 for forest and 0.33 for herbaceous vegetation (Kirdyashev et al., 1979).

A calibration procedure of the C-MEB model was conducted to account for the spatial variability of roughness parameters in West Africa which can play a significant role on the soil microwave emission. Simulations were done using the C-MEB model for a large range of the four soil parameter values (h_{soil}, q_{soil}, w_0 and bw_0) using the EPSAT-SG rainfall product from June to September 2006. Based on the root mean square errors (RMSE) between simulated and AMSR-E observed TB, it was shown that the two parameters related to the effective temperature have a minor impact on TB simulations. On the other hand, h_{soil} and q_{soil} parameters have a strong impact on TB simulations and a large dispersion of the two roughness parameters was found as shown in Fig. 6. The h_{soil} and q_{soil} maps are relevant with the presence of topography (Mountains of Aïr, Tibesti, and south of the Hoggar). In the South of the domain, covered with vegetation, the dispersion of the h_{soil} and q_{soil} values is due to a mixed contribution of soil roughness, topography and vegetation.

An example of estimated surface soil moisture mapping and associated simulated brightness temperatures (H-polarization) is shown in Fig. 7 for the 9 August 2006 01:30 a.m. In the same figure is shown the corresponding AMSR-E measurements (descending track, 9 August 2006 01:38 a.m.). A general agreement can be observed between the simulated and observed TB due to a significant rain system that wet a large part of the Sahel, from the South of the Aïr Mountains (Niger), to the Southern Mali, through North Mali. However, a detailed observation of the simulated TB signature exhibits some significant differences from the AMSR-E one. For instance, soil moisture simulations (and associated TB) display a wet area in North-Western Mali

(centred on ~4° E, 19° N) whereas no signature of a wet area can be observed in the AMSR-E measurements. Also shown in Fig. 7b is the vegetation optical thickness calculated using Eq. (7) which describes regions where the vegetation cover is important.

3.3 AMSR-E assimilation

The assimilation technique described in this study consists on obtaining simulated TB in agreement with observed TB by adjusting the rainfall accumulation estimate between two successive AMSR-E TB measurements. The initial rainfall accumulation estimate (EPSAT-SG) is modified using a multiplicative factor ranging from 0 to 7. The best solution is given by the rainfall rate which minimizes the difference between observed and simulated TB.

3.3.1 Results of the assimilation technique at the locale scale

First results of the assimilation technique generate some significant overestimations of the soil moisture which can last a long time after an important rainfall event. In order to avoid this problem, a second value of the δ decreasing time parameter is proposed to allow a rapid decrease of the soil moisture. The rapid decrease (δ=2880 min, i.e. 2 days) of the soil moisture is proposed only in case where no rain event occurs between two AMSR-E measurements. This is to avoid ambiguous results provided by either a significant rainfall associated with a rapid decrease of the soil moisture, or a small rainfall associated with a slow decrease of the soil moisture. Results at the locale scale are shown in Fig. 8 and statistical scores (R^2, RMSE and bias) are presented in Table 1.

It can be observed that the assimilation technique significantly increases the agreement between observed and simulated soil moisture at the Wankama site. Coefficient of determination (R^2) increases from 0.28 to 0.59. In addition, the soil moisture variations that were limited to the range 0.03 to 0.15 $m^3\,m^{-3}$ before assimilation are now more in agreement with the ground measurements (0.01 to 0.28 $m^3\,m^{-3}$). Finally, the

HESSD
6, 4035–4064, 2009

best improvement can be observed at the beginning of July and at the end of September where most of the unrealistic EPSAT-SG rainfalls which produced soil moisture variations were removed by the assimilation technique.

At the Agoufou site, the improvement is weaker. R^2 coefficient increases from 0.36 to 0.38. The soil moisture variations at the beginning and the end of the rainy season are in better agreement with observations. On the other hand, a minor rainfall event (5 September, 2 mm at the ground level) is overestimated by the assimilation technique. This behaviour might be explained by the different space scales used in the comparison and should constitute a limitation of the methodology. Ground measurements (soil moisture probes) were obtained at the plot scale whereas the assimilation technique is based on the AMSR-E measurements which are $25 \times 20\,km^2$ resolution. Thus, a large rainfall system can produce a small amount of rainfall at the periphery of the system and consequently causes an overestimation of the soil moisture at the ground measurement location.

Another limitation of the methodology was found at the Nalohou site and is related to the vegetation attenuation on microwave emission. As the vegetation cover increases (at the end of the rainy season), the sensitivity to soil moisture decreases. A sensibility test was conducted at the Nalohou site in Benin to define the vegetation optical depth threshold (τ_{max}) for which the surface soil moisture becomes negligible. A value of τ_{max} equal to 2.4 was found and corresponds to the 20 August date at the Nalohou site. Note that τ_{max} is equal to $\tau_{nadir}\,cos\theta$, with θ the satellite incidence angle (55° for AMSR-E), which corresponds to τ_{nadir} equal to 1.38. A modification of the assimilation technique was introduced and states that the assimilation is stopped when the optical thickness of the vegetation exceeds 2.4. In such cases, the original rainfall rate is used and no modification of the rainfall rate is allowed. Results of the second assimilation technique are shown in Fig. 9 and scores are presented in Table 1. Note that the second assimilation technique has no effect on the Wankama and Agoufou sites since the optical thickness of the vegetation never exceed 2.4 at these locations. Using the optical thickness threshold the R^2 coefficient increases from 0.35 to 0.51 at the

HESSD
6, 4035–4064, 2009

Nalohou site.

3.3.2 Results of the assimilation technique at the regional scale

The assimilation technique was applied at the regional scale. Surface soil moisture mapping and associated simulated brightness temperatures (H-polarization) for the 9 August 2006 01:30 a.m. are presented in Fig. 10. Also shown in Fig. 10b is the vegetation optical thickness calculated using Eq. (7), and the observed AMSR-E TB (d). First, it can be observed the excellent agreement between observed and simulated TB. This is not surprising since the assimilation technique selects the closest TB from the observed AMSR-E TB. The pattern of the wet area is now close to the observed one and wet areas at the East of the domain and in North Mali have been removed. Consequently, it can be observed that the soil moisture mapping (10a) is significantly different from the original one shown in Fig. 7a. Similarly to Fig. 7, the vegetation optical thickness is shown as well as the AMSR-E TBh measurements.

3.3.3 Rainfall accumulation estimates provided by the assimilation technique

The aims of this study deals with providing accurate surface soil moisture mapping with a fine temporal and spatial resolution over West Africa. To reach this goal, the proposed methodology modulates a rainfall accumulation product in order to match observed and simulated soil microwave emission. After assimilation, a new rainfall accumulation product is obtained and is compared to ground-based rainfall measurements in Fig. 11.

At the Wankama site, the total rainfall accumulation increases from 352 mm (EPAST-SG) to 538 mm (after assimilation). The total rainfall accumulation measured at the ground-level was 562 mm. In addition, there was 86 rainy days (d) in the EPSAT-SG product and the new number of rainy days decreases to 63 d whereas the number of rainy days measured at the ground-level was 34 d.

At the Agoufou site, the total rainfall accumulation increases from 307 mm (EPAST-SG) to 480 mm (after assimilation) whereas the total rainfall accumulation measured at

the ground-level was 358 mm. Although the number of rainy days decrease from 76 d to 54 d (39 d at the ground-level), the total rainfall accumulation is strongly overestimated by the methodology.

At the Nalohou site, the total rainfall accumulation as well as the number of rainy days is improved by the methodology as shown in Fig. 11c.

The explanation of the strong overestimation of the rainfall rate at the Agoufou site was investigated and was found to be related to the time period between two successive AMSR-E measurements which can last more than 30 h. Thus, a rainfall event which occurs 24 to 30 h before one AMSR-E measurement has a very weak signature or even no signature at all, as already observed by Pellarin et al. (2008). Consequently, the amount of rainfall has almost no influence on the soil emission 30 h later. Thus, the assimilation technique can select a large multiplicative factor which can be erroneous. This is particularly true in Mali where atmospheric conditions can produce significant evaporation rate after a rainy event.

4 Conclusions

This paper provides an original and simple methodology to map surface soil moisture with a fine temporal and spatial resolution over large areas based on the use of a rainfall accumulation product and soil microwave emission at C-band. The methodology accounts for the rainfall uncertainties associated to all satellite-based rainfall products. A methodology was developed to assimilate AMSR-E C-band measurements into an Antecedent Precipitation Index model coupled with a microwave emission model.

The methodology was assessed at the local scale using ground soil moisture measurements. A first limitation of the methodology was found to be related to the strong attenuation of the vegetation cover at C-band over forested areas (South of the domain). When the optical thickness of the vegetation exceed 2.4 (which means 1.38 at nadir), the assimilation technique was found to be helpless. A second limitation was related to the possible underestimation or overestimation of a rain event provided by

the assimilation technique due to the different spatial resolution between the precipitation product and the microwave emission measurements. This limitation prevents the methodology to provide simultaneously a soil moisture mapping and a rainfall accumulation mapping. The first limitation was solved using a threshold on the optical thickness of the vegetation and led to improve the soil moisture retrieval at the Nalohou site in Benin. No modification was proposed to solve the second limitation which concerns only few days essentially in Mali.

In term of perspectives, these soil moisture maps will be used to study the potential role of the soil moisture in the initiation of the convection in the Sahel. In addition, in the frame of the SMOS mission, these maps will be helpful in the Calibration/Validation procedure which will take place in summer 2010 in West Africa. It is also planed to improve the methodology in order to correct the precipitation rate using satellite-based soil moisture measurements as suggested in Crow and Bolten (2007) and Crow et al. (2009).

Acknowledgements. Based on a French initiative, AMMA was built by an international scientific group and is currently funded by a large number of agencies, especially from France, the UK, the US and Africa. It has been the beneficiary of a major financial contribution from the European Community's Sixth Framework Research Programme. Detailed information on scientific coordination and funding is available on the AMMA International web site http://www.amma-international.org.

The authors wish to thank NSIDC for providing us with AMSR-E/Aqua daily L3 surface soil moisture data (Njoku, E., updated daily. AMSR-E/Aqua daily L3 surface soil moisture, interpretive parms, & QC EASE-Grids, Junuary to December 2006. Boulder, CO, USA: National Snow and Ice Data Center. Digital media)

The publication of this article is financed by CNRS-INSU..

References

Adler, R. F., Huffman, G. J., Chang, A., Ferraro, R., Xie, P. P., Janowiak, J., Rudolf, B., Schneider, U., Curtis, S., Bolvin, D., Gruber, A., Susskind, J., Arkin, P., and Nelkin, E.: The version-2 global precipitation climatology project (GPCP) monthly precipitation analysis (1979-present). J. Hydrometeorol., 4, 1147–1167, 2003.

Boone A., de Rosnay, P., Balsamo, G., Beljaars, A., Chopin, F., Decharme, B., Delire, C., Ducharne, A., Gascoin, S., Guichard, F., Gusev, Y., Harris, P., Jarlan, L., Kergoat, L., Mougin, E., Nasonova, O., Norgaard, A., Orgeval, T., Ottlé, C., Poccard-Leclercq, I., Polcher, J., Sandholt, I., Saux-Picart, S., Taylor, C. M., and Xue, Y.: The AMMA Land Surface Model Intercomparison Project (ALMIP), B. Am. Meteorol. Soc., in revision, 2008.

Cheng, W. Y. Y. and Cotton, W. R.: Sensitivity of a cloud-resolving simulation of the genesis of a mesoscale convective system to horizontal heterogeneities in soil moisture initialization, J. Hydrometeorol., 5, 934–958, 2004.

Chopin, F., Bergès, J. C., Desbois, M., Jobard, I., and Lebel, T.: Satellite Rainfall Probability and Estimation. Application to the West Africa During the 2004 Rainy Season, American Geosciences Union, 2005 Joint Assembly New Orleans, USA, 23–27 May 2005.

Cook, B. I., Bonan, G. B., and Levis, S.: Soil moisture feedbacks to precipitation in southern Africa, J. Climate, 19, 4198–4206, 2006.

Crow, W. T. and Bolten, J. D.: Estimating precipitation errors using spaceborne surface soil moisture retrievals, Geophys. Res. Lett., 34(8), L08403, doi:10.1029/2007GL029450, 2007.

Crow, W. T., Huffman, G. J., Bindlish, R., and Jackson, T. J.: Improving Satellite-Based Rainfall Accumulation Estimates Using Spaceborne Surface Soil Moisture Retrievals, J. Hydrometeorol., 10, 199–212, 2009.

Crow, W. T. and Ryu, D.: A new data assimilation approach for improving runoff prediction using remotely-sensed soil moisture retrievals, Hydrol. Earth Syst. Sci., 13, 1–16, 2009, http://www.hydrol-earth-syst-sci.net/13/1/2009/.

de Rosnay, P., Gruhier, C., Timouk, F., Baup, F., Mougin, E., Hiernaux, P., Kergoat, L., and LeDantec, V.: Multi-scale soil moisture measurements at the Gourma meso-scale site in Mali, J. Hydrol., doi:10.1016/j.jhydrol.2009.01.015, 2009a.

de Rosnay, P., Drusch, M., Boone, A., Balsamo, G., Decharme, B., Harris, P., Kerr, Y., Pellarin,

T., Polcher, J., and Wigneron, J.-P.: The AMMA Land Surface Model Intercomparison Experiment coupled to the Community Microwave Emission Model: ALMIP-MEM, J. Geophys. Res., 114, D05108, doi:10.1029/2008JD010724, 2009b

Entekhabi, D., Njoku, E. G., O'Neill, P. E., Jackson, T. J., Boland, S. W., and Entin, J. K.: The Soil Moisture Active/Passive Mission (SMAP), edited by: E. T. AGU, 2007 Fall Meeting, 2007.

Jackson, T. J., Moran, M. S., and O'Neill, P. E.: Introduction to Soil Moisture Experiments 2004 (SMEX04) Special Issue, Remote Sens. Environ., 112, 301–303, 2008.

Kerr, Y. H., Waldteufel, P., Wigneron, J. P., Martinuzzi, J. M., Font, J., and Berger, M.: Soil moisture retrieval from space: The Soil Moisture and Ocean Salinity (SMOS) mission, IEEE T. Geosci. Remote, 39, 1729–1735, 2001.

Kirdyashev, K. P., Chukhlantsev, A. A., and Shutko, A. M.: MICROWAVE RADIATION OF GROUNDS WITH VEGETATIVE COVER, Radiotekh. Elektron.+, 24, 256–264, 1979.

Koster, R. D., Dirmeyer, P. A., Guo, Z. C., Bonan, G., Chan, E., Cox, P., Gordon, C. T., Kanae, S., Kowalczyk, E., Lawrence, D., Liu, P., Lu, C. H., Malyshev, S., McAvaney, B., Mitchell, K., Mocko, D., Oki, T., Oleson, K., Pitman, A., Sud, Y. C., Taylor, C. M., Verseghy, D., Vasic, R., Xue, Y. K., Yamada, T., and Team, G.: Regions of strong coupling between soil moisture and precipitation, Science, 305, 1138–1140, 2004.

Laurent, H., Jobard, I., and Toma, A.: Validation of satellite and ground-based estimates of precipitation over the Sahel, in: 12th International Conference on Clouds and Precipitation, Zurich, Switzerland, 651–670, 1996.

Liu, Y. Q. and Avissar, R.: A study of persistence in the land-atmosphere system using a general circulation model and observations, J. Climate, 12, 2139–2153, 1999.

Masson, V., Champeaux, J. L., Chauvin, F., Meriguet, C., and Lacaze, R.: A global database of land surface parameters at 1-km resolution in meteorological and climate models, J. Climate, 16, 1261–1282, 2003.

Mathon, V., Laurent, H., and Lebel, T.: Mesoscale convective system rainfall in the Sahel, J. Appl. Meteorol., 41, 1081–1092, 2002.

Mironov, V. L., Dobson, M. C., Kaupp, V. H., Komarov, S. A., and Kleshchenko, V. N.: Generalized refractive mixing dielectric model for moist soils, IEEE T. Geosci. Remote, 42, 773–785, 2004.

Mo, T., Choudhury, B. J., Schmugge, T. J., Wang, J. R., and Jackson, T. J.: A MODEL FOR MICROWAVE EMISSION FROM VEGETATION-COVERED FIELDS, J. Geophys. Res.-Oc.

Atm., 87, 1229–1237, 1982.
Noilhan, J. and Planton, S.: A SIMPLE PARAMETERIZATION OF LAND SURFACE PROCESSES FOR METEOROLOGICAL MODELS, Mon. Weather Rev., 117, 536–549, 1989.
Pellarin, T., Ali, A., Chopin, F., Jobard, I., and Berges, J. C.: Using spaceborne surface soil moisture to constrain satellite precipitation estimates over West Africa, Geophys. Res. Lett., 35(2), L02813, doi:10.1029/2007GL032243, 2008.
Pellarin, T., Calvet, J. C., and Wigneron, J. P.: Surface soil moisture retrieval from L-band radiometry: A global regression study, IEEE T. Geosci. Remote, 41, 2037–2051, 2003.
Pellarin, T., Kerr, Y. H., and Wigneron, J. P.: Global simulation of brightness temperatures at 6.6 and 10.7 GHz over land based on SMMR data set analysis, IEEE T. Geosci. Remote, 44, 2492–2505, 2006.
Pellarin, T., Laurent, J.-P., Cappelaere, B., Decharme, B., Descroix, L., and Ramier, D.: Hydrological modelling and associated microwave emission of a semi-arid region in South-western Niger, J. Hydrol., doi:10.1016/j.jhydrol.2008.12.003, 2009.
Prigent, C., Aires, F., Rossow, W. B., and Robock, A.: Sensitivity of satellite microwave and infrared observations to soil moisture at a global scale: Relationship of satellite observations to in situ soil moisture measurements, J. Geophys. Res.-Atmos., 110(D7), D07110, doi:10.1029/2004JD005087, 2005.
Taylor, C. M. and Ellis, R. J.: Satellite detection of soil moisture impacts on convection at the mesoscale, Geophys. Res. Lett., 33(3), L03404, doi:10.1029/2005GL025252, 2006.
Taylor, C. M., Said, F., and Lebel, T.: Interactions between the land surface and mesoscale rainfall variability during HAPEX-Sahel, Mon. Weather Rev., 125, 2211–2227, 1997.
Wang, J. R., Oneill, P. E., Jackson, T. J., and Engman, E. T.: MULTIFREQUENCY MEASUREMENTS OF THE EFFECTS OF SOIL-MOISTURE, SOIL TEXTURE, AND SURFACE-ROUGHNESS, IEEE T. Geosci. Remote, 21, 44–51, 1983.
Wigneron, J. P., Kerr, Y., Waldteufel, P., Saleh, K., Escorihuela, M. J., Richaume, P., Ferrazzoli, P., de Rosnay, P., Gurney, R., Calvet, J. C., Grant, J. P., Guglielmetti, M., Hornbuckle, B., Matzler, C., Pellarin, T., and Schwank, M.: L-band Microwave Emission of the Biosphere (L-MEB) Model: Description and calibration against experimental data sets over crop fields, Remote Sens, Environ,, 107, 639–655, 2007.
Wigneron, J. P., Laguerre, L., and Kerr, Y. H.: A simple parameterization of the L-band microwave emission from rough agricultural soils, IEEE T. Geosci. Remote, 39, 1697–1707, 2001.

Table 1. Statistical scores of the soil moisture estimates for the three locale scale sites. Simulations were done using **(a)** ground-based rainfall estimates, **(b)** EPSAT-SG rainfall estimates and **(c)** EPSAT-SG rainfall estimates with assimilation technique. **(d)** corresponds to the assimilation technique performed with the τ_{max} threshold.

		Ground rainfall (a)	EPSAT-SG rainfall (b)	Assimilation (c)	Assimilation (d)
Wankama	R^2	0.69	0.28	0.59	
	RMSE (%vol.)	1.9	3.1	2.9	
	Bias (%vol.)	−0.5	−0.9	−1.3	unchanged
	Rainy days	34	86	63	
Agoufou	R^2	0.63	0.36	0.38	
	RMSE (%vol.)	2.1	3.1	3.1	
	Bias (%vol.)	−1.0	−0.4	−0.7	unchanged
	Rainy days	39	76	54	
Nalohou	R^2	0.50	0.46	0.35	0.51
	RMSE (%vol.)	3.3	3.7	3.7	3.1
	Bias (%vol.)	−0.1	1.6	1.0	0.3
	Rainy days	51	97	84	86

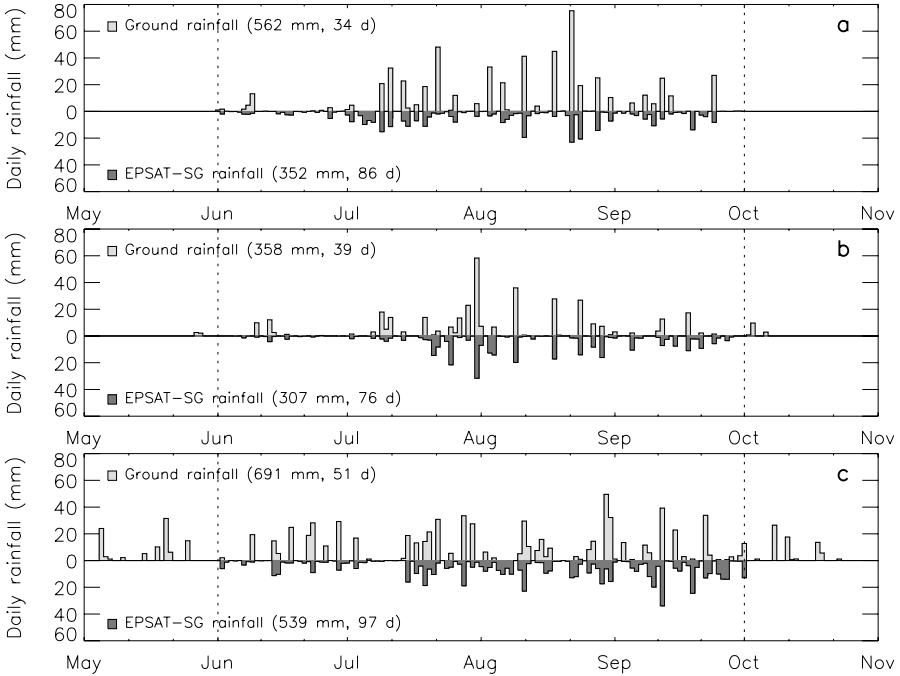

Fig. 1. Daily rainfall products (2006) over Niger **(a)**, Mali **(b)** and Benin **(c)**. Reference rainfalls (measured using raingauge stations) are plotted in light histograms and EPSAT-SG rainfalls are plotted in dark histograms. The total rainfall amount and the number of rainy days are indicated.

HESSD
6, 4035–4064, 2009

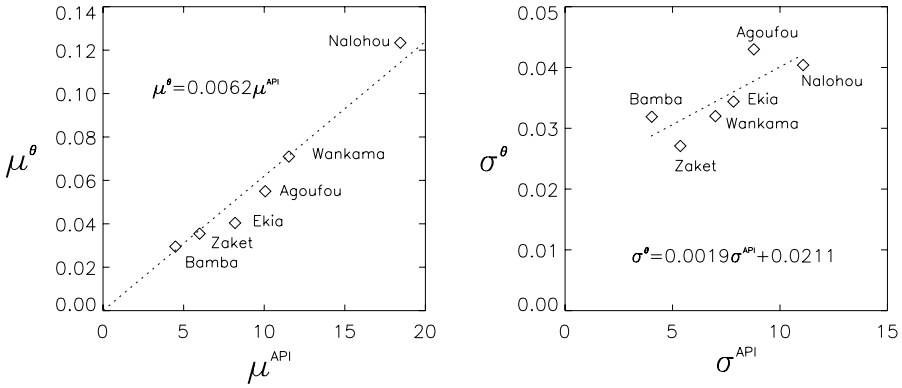

Fig. 2. (a) statistical relationship between mean API (June–September) and mean surface soil moisture measured over six sites. **(b)** Same as (a) but concerning standard deviation.

HESSD
6, 4035–4064, 2009

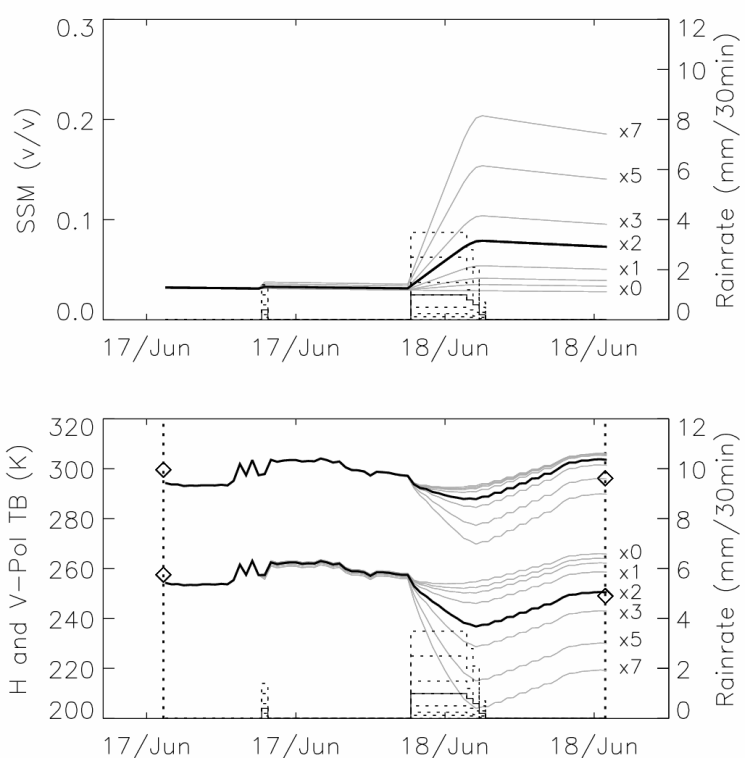

Fig. 3. Illustration of the methodology based on the selection of the best precipitation rate which minimizes the difference between AMSR-E TB observations (diamonds in the lower graph) and simulated TB. Here, the best TB simulation is obtained using a multiplicative factor of 2 on the precipitation rate (Niger site).

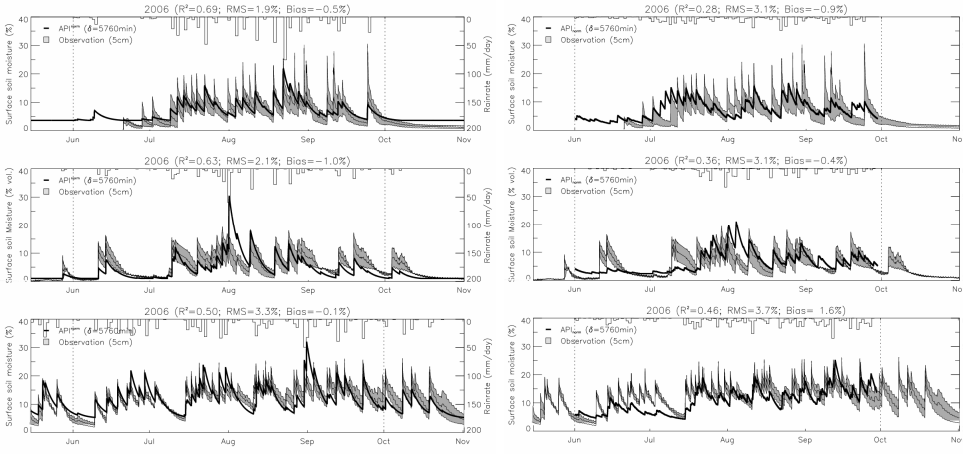

Fig. 4. Observed (gray areas) and estimated surface soil moisture (black thick lines) during 2006 over three sites (Wankama, Agoufou and Nalohou) using API model and ground-based rainfall measurements (left 3 graphs) and satellite-based rainfall estimates (right 3 graphs).

HESSD
6, 4035–4064, 2009

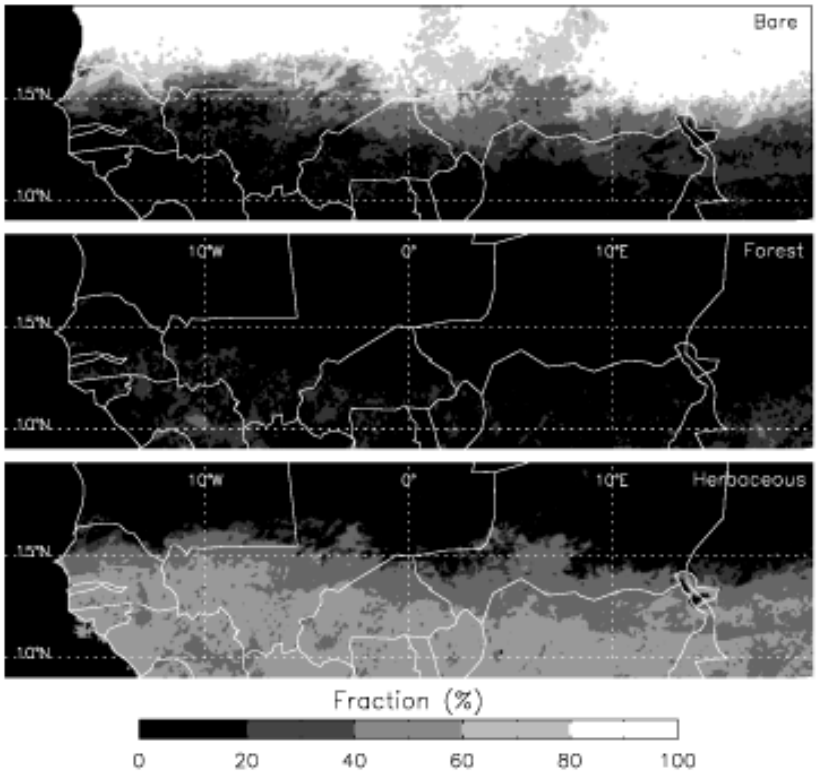

Fig. 5. Soil fraction used for the microwave TB simulation: bare soil fraction (top), forest fraction (middle) and herbaceous vegetation fraction (bottom).

HESSD

6, 4035–4064, 2009

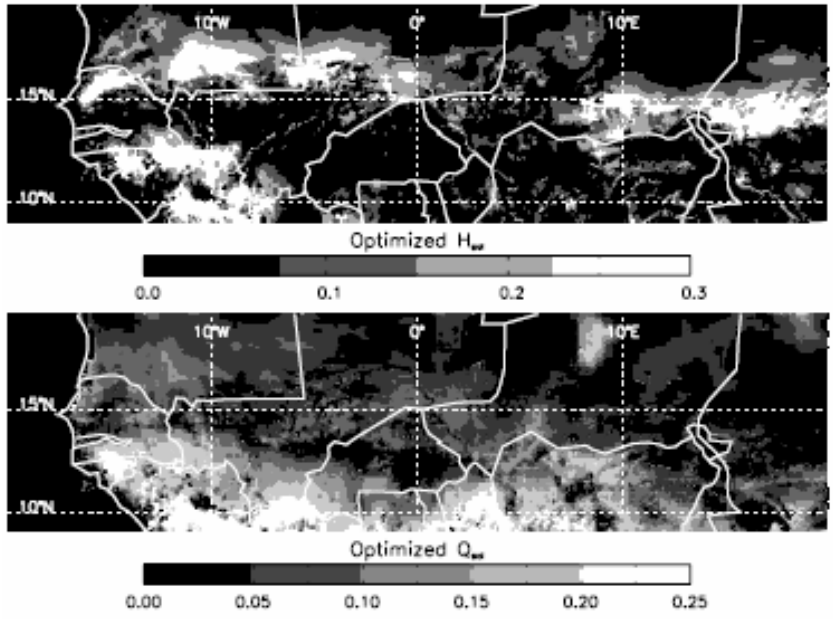

Fig. 6. Soil roughness parameter (h_{soil} and q_{soil}) mapping obtained by a calibration procedure based on AMSR-E TB measurements and the C-MEB model.

HESSD
6, 4035–4064, 2009

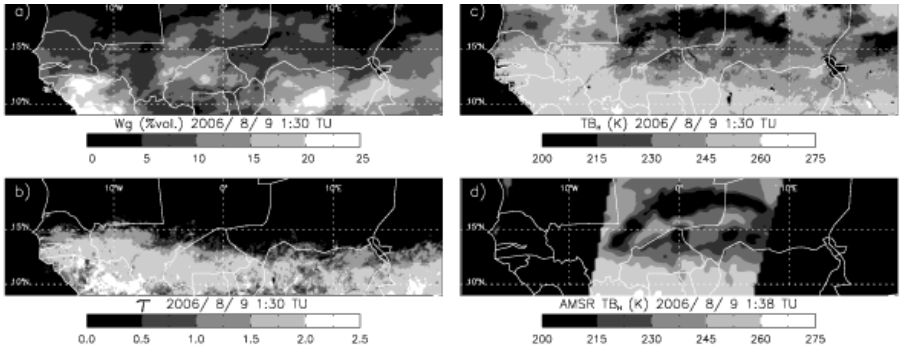

Fig. 7. Surface soil moisture mapping **(a)** obtained using the API model and the EPSAT-SG rainfall accumulation product. **(b)** Presents the vegetation optical depth at C-band obtained using Eq. (7) and VWc provided by the ECOCLIMAP database. The two right-graphs present the simulated TB **(c)** and the corresponding AMSR-E TB **(d)** at horizontal polarization for the same date (9 August 2006, 01:38 a.m.).

HESSD
6, 4035–4064, 2009

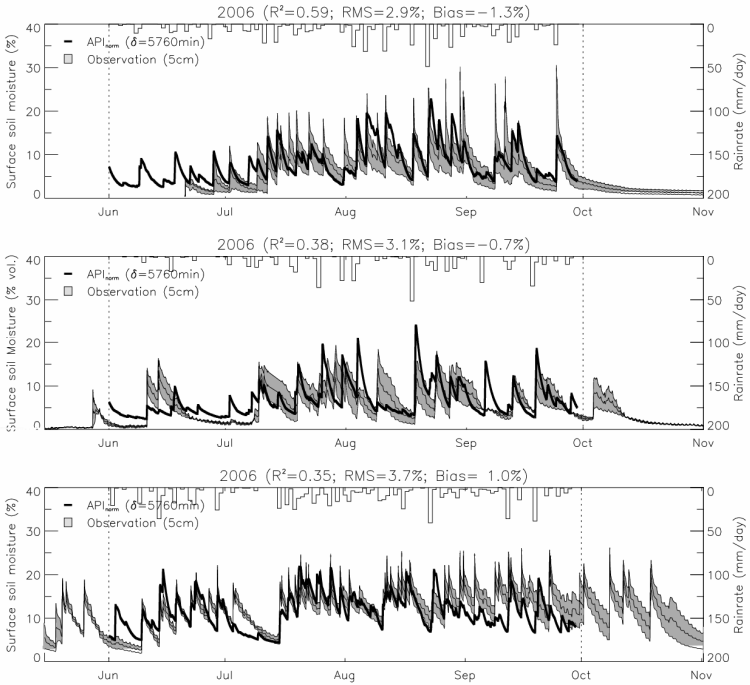

Fig. 8. Observed (gray area) and estimated surface soil moisture (2006) over three sites (Wankama, Agoufou and Nalohou) after assimilation of the AMSR-E TB measurements. Histograms present the obtained rainfall accumulation after the assimilation technique.

HESSD
6, 4035–4064, 2009

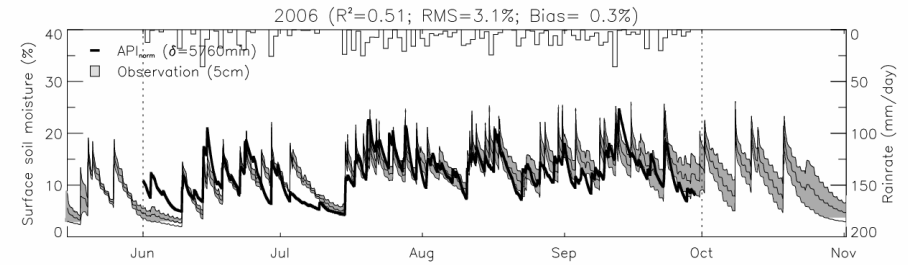

Fig. 9. Result of the assimilation technique over the Nalohou site using the τ_{max} threshold. When the vegetation optical thickness at 55° incidence angle exceeds 2.4, the rainfall modification is not allowed.

HESSD
6, 4035–4064, 2009

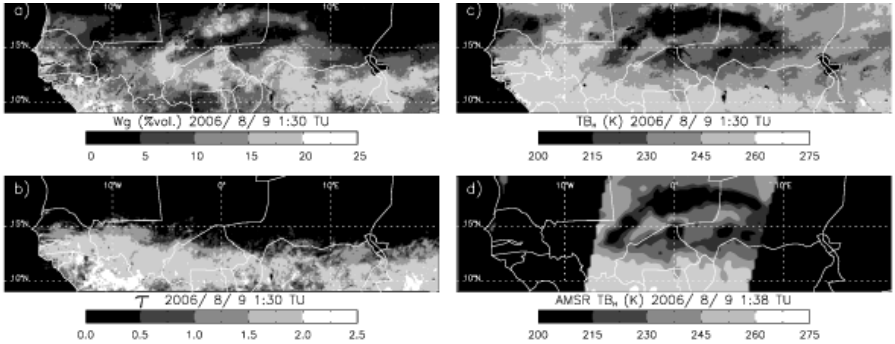

Fig. 10. Same as Fig. 7 but after the assimilation procedure.

HESSD
6, 4035–4064, 2009

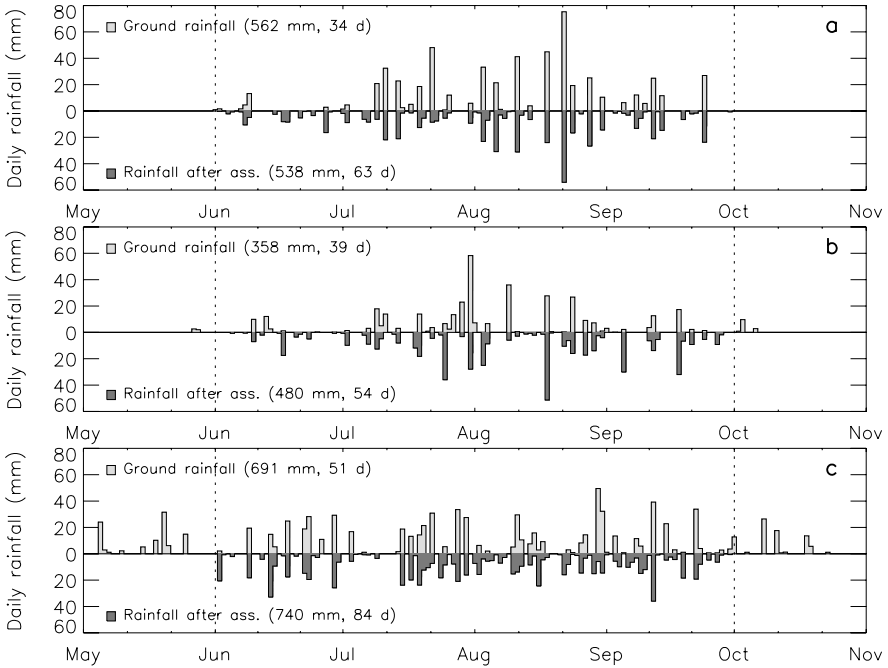

Fig. 11. Daily rainfall products (2006) over Niger **(a)**, Mali **(b)** and Benin **(c)**. Reference rainfalls (measured using raingauge stations) are plotted in light histograms and low-axis values represent the rainfall product provided by the assimilation technique. The total rainfall amount and the number of rainy days are indicated.

HESSD
6, 4035–4064, 2009